The Performance And Clock Error Prediction Analysis of BDS Satellite Clock: A Comparison between BDS-2 And BDS-3

Dong Zhenghua[1*]

[1]Student, College of Surveying and Geo-informatics, Tongji University, 1239 Siping Road, Shanghai, China

*dbxjlhp@126.com

Abstract: *To study the performance of BDS satellite atomic clocks and the accuracy of satellite clock error prediction, and to compare the difference between BeiDou Regional Navigation Satellite System (BDS-2) and BeiDou Global Navigation Satellite System (BDS-3). On the basis of analyzing the noise, frequency drift and frequency stability of satellite atomic clocks with a time span of one year from June 2023 to May 2024, three clock error prediction models, namely quadratic polynomial (QP), grey model (GM), and autoregressive integrated moving average (ARIMA), were selected to fit and predict based on the data of 7 days. Compared with BDS-2, BDS-3 atomic clocks have a lower noise level, with the average annual noise levels of BDS-2 rubidium clock, BDS-3 new rubidium clock, and BDS-3 hydrogen clock reaching 0.80 ns, 0.68 ns and 0.19 ns, respectively. Similarly, the BDS-3 atomic clocks have a better satellite clock frequency drift, with the annual frequency drifts of BDS-2 rubidium clock, BDS-3 new rubidium clock, and BDS-3 hydrogen clock can achieve values of* 11.57×10^{-19}, 3.01×10^{-19} *and* 1.57×10^{-19}*, respectively. In contrast to BDS-2, BDS-3 atomic clocks have higher frequency stability. Specifically, the ten thousand seconds stabilities of BDS-2 rubidium clock, BDS-3 new rubidium clock, and BDS-3 hydrogen clock are* 4.25×10^{-14}, 1.36×10^{-14} *and* 1.35×10^{-14}*, respectively. The prediction accuracy of BDS-3 hydrogen clock, and BDS-3 new rubidium clock have been significantly improved in comparison with the BDS-2 rubidium clock. Moreover, for ARIMA model, the prediction accuracy of BDS-3 hydrogen clock at 3 h, 6 h and 12 h can respectively reach 0.19 ns, 0.26 ns and 0.33 ns. For BDS satellite clock, ARIMA has the highest prediction accuracy and prediction stability, the prediction accuracy and prediction stability of GM are better than that of QP. But for BDS-3 new rubidium clock, QP has the better prediction accuracy and prediction stability than GM. By this study, we can understand the performance and the clock error prediction accuracy of BDS satellite clock, the difference between BDS-2 and BDS-3, and provide useful references for modeling and refining the BDS satellite clock error.*

Keywords: BDS-2, BDS-3, performance, prediction

Introduction

The BeiDou Navigation Satellite System (BDS) is an independent and autonomous Global Navigation Satellite System (GNSS) established by China, comprising three satellite navigation subsystems: BeiDou Experimental Navigation Satellite System (BDS-1), BeiDou Regional Navigation Satellite System (BDS-2), and BeiDou Global Navigation Satellite System (BDS-3). The construction of the BDS-1 commenced in 1994, and the system was completed and put into operation in 2000, providing positioning, timing, wide-area differential, and short-message communication services to Chinese users. This navigation satellite system has since been decommissioned. In 2004, the construction of the BDS-2 was initiated, and by 2012, the network formation of 14 satellites was accomplished, offering positioning, velocity measurement, timing, wide-area differential, and short-message communication services to users in the Asia-Pacific region. The construction of the BDS-3 began in 2009, with basic services extended to countries and regions along the Belt and Road Initiative (BRI) starting in 2018. On July 31, 2020, the BDS-3 was officially inaugurated.

Compared to BDS-2, BDS-3 has upgraded its regional service capabilities to provide global navigation and positioning services, with enhanced performance. In terms of satellite payloads, BDS-3 employs new rubidium atomic clock and new hydrogen atomic clock, further improving the satellites' performance and operational lifespan (Guo et al., 2019).

Global navigation positioning systems are based on time measurement, where accurate distance measurement fundamentally relies on precise time measurement. Onboard atomic clocks serve as the time references for navigation positioning and are among the core payloads of navigation satellites, with their performance directly influencing the precision of navigation and positioning. Evaluations of onboard atomic clocks' noise, frequency drift, and frequency stability are crucial for both the maintenance and monitoring of the timing system and for the prediction and estimation of satellite clock error. Moreover, clock error prediction plays a significant role in enhancing the accuracy of real-time positioning.

Scholars have conducted a lot of researches on the performance analysis of GNSS satellite clock. Senior et al. (2008) conducted a long-term analysis of GPS onboard atomic clocks, revealing that atomic clocks exhibit periodicity and providing guidance for refining clock error prediction models. Hauschild et al. (2013) conducted a short-term study on the stability of spaceborne atomic clocks using Kalman filtering and polynomial fitting methods. Wang et al. (2017) conducted frequency stability analysis on atomic clocks of BDS system, but they only selected a subset of BDS satellites and did not evaluate all BDS satellites. Jiang et al. (2019) evaluated the long-term in-orbit performance of BDS-2 onboard atomic clocks using five and a half years of clock error data. Mao et al. (2020) conducted periodic and stability analyses on the atomic clocks of BDS-3. Kan et al. (2021) performed medium to long-term analyses of BDS-3 onboard atomic clocks under various time synchronization systems, demonstrating that the frequency accuracy and frequency drift evaluated by the three clock error determination systems are essentially consistent.

Commonly used clock error prediction models include autoregressive integrated moving average (ARIMA), grey models (GM), linear polynomial (LP) models, and quadratic polynomial (QP) models, among others (Xi et al., 2014; Li et al., 2016; Huang et al., 2018). Due to the varying adaptability of these models and the influence of external environmental factors and intrinsic characteristics on atomic clocks, it is challenging to identify a clock error prediction model suitable for all GNSS satellites. A great deal of scholars have conducted researches on the prediction model of GNSS clock error. Panfilo et al. (2008) focused on the noise characteristics of clock error, proposing a satellite clock error prediction model that incorporates random walk noise. Zheng et al. (2008) addressed the limitations of traditional GM by improving it and utilizing the enhanced model to prediction clock error for different types of satellites over varying durations. Allan et al. (2016) employed statistical methods to investigate clock error prediction. In recent years, some scholars have achieved high prediction accuracy using machine learning for satellite clock error prediction. However, machine learning methods require the setting of numerous parameters, and the selection of these parameters lacks a scientific theoretical basis (Wang et al., 2021; Meng et al., 2022).

In summary, research on BDS onboard atomic clocks has predominantly focused on BDS-2, while studies on BDS-3 satellite clock lack analyses of newer data, insufficiently explore the long-term characteristics of BDS-3 atomic clocks, and are deficient in comparative analyses between BDS-2 and BDS-3.

Given the above analysis, this study, based on the analysis of satellite clock performance (noise, frequency drift, and frequency stability) of BDS satellite clock, employs three clock error prediction models (QP, GM, ARIMA) to fit and predict clock errors. It summarizes the prediction accuracy of different types of atomic clocks and evaluates the stability of the prediction models. Meanwhile, the differences between BDS-2 and BDS-3 were compared and analyzed.

Methodology

The noise, frequency drift, and frequency stability of satellite clock are important indicators for analyzing their performance. Predicting satellite clock error is of significant importance for real-time navigation and positioning applications. However, the prediction accuracy is influenced by multiple factors, including the suitability of the models and the performance quality of the atomic clocks.

Therefore, to objectively analyze the performance of BDS satellite clock and the accuracy of clock error prediction, this study investigates the noise, frequency drift, and frequency stability of the atomic clocks, and conducts a comparative analysis of three clock error prediction models. This approach not only evaluates the performance of the satellite clock but also provides useful references for selecting appropriate models for clock error prediction.

Satellite Clock Noise

As onboard reference for generating navigation signal and performing ranging, satellite clock directly determines the accuracy of the satellite's time and frequency, and consequently, the overall service performance of the entire navigation satellite system. To more accurately assess the performance of satellite clock, it is essential to first perform noise analysis on the satellite clock.

A quadratic polynomial fitting is applied to data from a single day, and the residual sequence from the daily fitting is statistically analyzed, treating the fitting residual as the noise of the satellite clock. The quadratic polynomial fitting formula is as follows:

$$x_i = a_0 + a_1(t_i - t_0) + a_2(t_i - t_0)^2 + \Delta_i \quad i = 1,2,\cdots,N \tag{1}$$

Where, x_i represents the satellite clock error, a_0 is the initial clock error, a_1 is the frequency, a_2 is the frequency drift, t_i is the epoch time, t_0 is the reference time, Δ_i is the model residual (Huang et al., 2017).

Satellite Clock Frequency Drift

Frequency drift refers to the numerical value representing how the nominal frequency changes over time. In navigation and positioning, onboard atomic clocks experience frequency drift due to aging of internal hardware as their operational time increases, leading to frequency drift phenomena. Frequency drift generally exhibits a linear trend, and the frequency drift value of satellite clock represents the rate of frequency change. There are generally two formulas for calculating the frequency drift: one involves fitting the frequency data using least squares, and the other involves quadratic polynomial fitting of clock error. The least squares fitting formula is as follows:

$$D = \frac{\sum_{i=1}^{N}[y_i(\tau) - \overline{y_i}(\tau)](t_i - \bar{t})}{\sum_{i=1}^{N}(t_i - \bar{t})^2} \tag{2}$$

$$\overline{y_i}(\tau) = \frac{1}{N}\sum_{i=1}^{N} y_i, \quad \bar{t} = \frac{1}{N}\sum_{i=1}^{N} t_i$$

Where, D is the frequency drift rate, $\mathrm{y_i}(\tau)$ is the frequency value at time $\mathrm{t_i}$, τ is the sampling interval, $\overline{\mathrm{y_i}}(\tau)$ is the mean of the 1 to N frequency data, $\bar{\mathrm{t}}$ is the mean of the 1 to N time data (Mao et al., 2011).

The quadratic polynomial fitting formula is as shown in Equation (1).

Satellite Clock Frequency Stability

Frequency stability is an indicator that measures the random fluctuations in the output frequency of a satellite atomic clock over a certain period of time. Therefore, frequency stability is not a fixed numerical value and will change over time. Generally, Allan variance and Hadamard variance are used to calculate frequency stability. Since Allan variance is typically used for statistical analysis of the frequency stability of cesium clock. The BDS is equipped with rubidium clock and hydrogen clock. Due to the significant frequency drift of rubidium clock, Hadamard variance is employed to analyze the frequency stabilities of atomic clocks in the BDS.

For a frequency data sequence $\mathrm{y_n}$, $\mathrm{n} = \{1,2,\ldots,\mathrm{M}\}$, with a sampling interval τ_0 and M being the number of samples, the Hadamard variance based on frequency data can be expressed as:

$$H\sigma_y^2(\tau) = \frac{1}{6(M\prime-2)}\sum_{i=1}^{M\prime-2}[\overline{y}_{i+2m}(m) - 2\overline{y}_{i+1m}(m) + \overline{y}_i(m)]^2 \tag{3}$$

Where, $\tau = m\tau_0$ is the smoothing time, m is the smoothing factor ($1 \leq m \leq \mathrm{int}(M/3)$), $M' = int(M/m) + 1$, $\overline{y_i}(m)$ is the mean of m frequency data (Mao et al., 2011).

Satellite Clock Error Prediction Methods

Polynomial Model

These models are typically constructed based on the time-frequency characteristics of atomic clocks, including phase, frequency, and frequency drift. They mainly include the LP model and the QP model. The QP model's equation is as shown in Equation (1).

Grey Model

The grey model is the process of sequentially accumulating the original time series to form a new sequence with distinct characteristic patterns, and then approximating it with the solution of a first-order linear differential equation (Li et al., 2016). The model is expressed as:

$$X^{(1)}(k+1) = \left[X^{(0)}(1) - \frac{\hat{\mu}}{\hat{\alpha}}\right] \cdot e^{-\hat{\alpha}k} + \frac{\hat{\mu}}{\hat{\alpha}} \tag{4}$$

Where, $X^{(0)} = \{X^{(0)}(1), X^{(0)}(2), \cdots, X^{(0)}(n)\}$ is the original clock error sequence, $X^{(1)} = \{X^{(1)}(1), X^{(1)}(2), \cdots, X^{(1)}(n-1)\}$ is the accumulated clock error sequence, $\hat{\mu}$ is the grey action quantity, reflecting the fluctuation of the sequence, $\hat{\alpha}$ is the grey coefficient, representing the evolution trend between sequences, e is the natural constant. The original clock error sequence $X^{(0)}(k)$ can be sequentially restored by subtracting as follows:

$$X^{(0)}(k) = X^{(1)}(k) - X^{(1)}(k-1) \tag{5}$$

ARIMA Model

The ARIMA model combines Autoregressive (AR) and Moving Average (MA) models and introduces differencing methods to handle non-stationary time series predicting. GNSS satellite clock error sequences exhibit significant non-stationary characteristics. The ARIMA model effectively eliminates trend and periodic components from non-stationary sequences through differencing, enabling modeling and predicting of the processed clock error sequences. The ARIMA (p, d, q) model is defined as $\{x_t\}$ ~ARIMA (p, d, q), where $\{x_t\}$ is the data sequence, p and q are the orders of the model, and d is the number of differences. When d=0, it reduces to the ARMA model:

$$x_t = \sum_{i=1}^{p} a_i x_{t-i} + \varepsilon_t + \sum_{j=1}^{q} b_j \varepsilon_{t-j} \tag{6}$$

Where, a_i and b_j are the autoregressive and moving average parameters, respectively, $\{\varepsilon_t\} \sim$ WN $(0, \sigma^2)$ is a white noise sequence with variance σ^2 (Xi et al., 2014).

Specific Experimental Method

1. Apply quadratic polynomial fitting to single-day data and statistically analyze the fitting residual (noise) over the entire year.

2. Apply quadratic polynomial fitting to single-day data to determine frequency drift and statistically assess the frequency drift accuracy over the entire year.

3. When evaluating the frequency stability of satellite atomic clock using Hadamard variance, continuous data is utilized for computation.

4. Based on 7 days of precise clock error data from Wuhan University (WHU), employ QP, GM, and ARIMA models to perform fitting and predicting of clock errors. Specifically, use the first 12 hours of clock error data each day for fitting and predict the subsequent 12 hours of satellite clock error, conducting accuracy analyses over predicting intervals of 3 hours, 6 hours, and 12 hours.

5. Due to the presence of abnormal data and data missing in the WHU precise clock error products, preprocessing of BDS satellite clock error data is necessary. Identifying outliers using the Median Absolute Deviation (MAD) method, and filling missing data through linear interpolation.

Results and Discussion

Experimental Data

The experimental data were selected from the WHU precise clock error products with a sampling interval of 30 seconds, spanning one year from June 2023 to May 2024. For the clock error fitting and predicting analysis, data from seven consecutive days, corresponding to the Day of Year (DOY)146 to 152 in 2024, were utilized from the WHU precise clock error products. Within the one-year timeframe, the WHU precise clock products include a total of 15 satellites for BDS-2 and 27 satellites for BDS-3. The 15 BDS-2 satellites are designated by the pseudo random noise codes (PRNs): C01, C02, C03, C04, C05, C06, C07, C08, C09, C10, C11, C12, C13, C14, C16, and all of them equipped with rubidium clock. The 27 BDS-3 satellites include 12 satellites designated by PRNs: C19, C20, C21, C22, C23, C24, C32, C33, C36, C37, C41, C42, which equipped with new rubidium clock, and 15 satellites designated by PRNs: C25, C26, C27, C28, C29, C30, C34, C35, C38, C39, C40, C43, C44, C45, C46, which equipped with hydrogen clock.

Satellite Clock Noise Analysis

Assuming June 1, 2023, as the DOY 1 and May 31, 2024, as the DOY 366, the following figures present the annual time series of noise variations for BDS-2 rubidium clock, BDS-3 new rubidium clock, and BDS-3 hydrogen clock. In Figures 1, 2, and 3, the vertical axes represent the noise (fitting residual) of each satellite at each epoch (30 seconds), and the horizontal axes represent the DOY. Figure 1 corresponds to BDS-2 rubidium clock, Figure 2 corresponds to BDS-3 new rubidium clock, and Figure 3 corresponds to BDS-3 hydrogen clock. Table 1 presents the annual root mean square (RMS) value of noise for each BDS satellite clock, providing statistical data on the annual noise levels of each satellite clock.

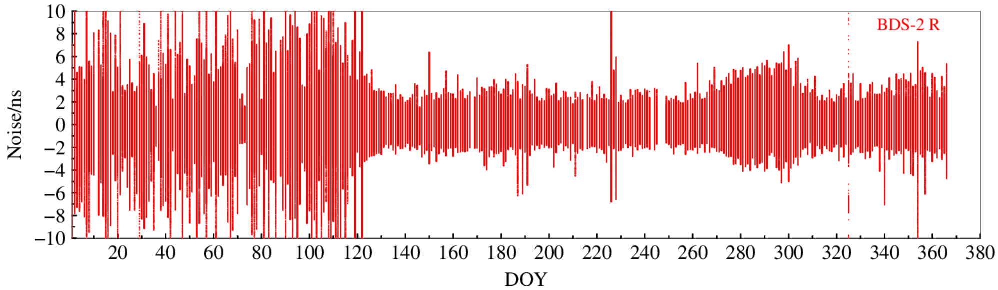

Figure 1: Time Series of Annual Noise of BDS-2 Satellite Rubidium Clock.

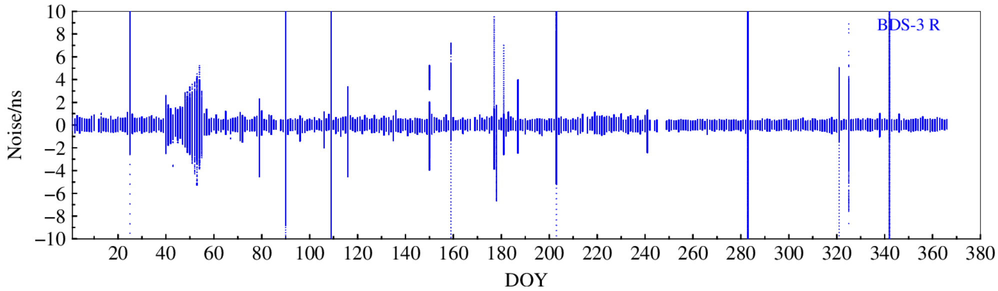

Figure 2: Time Series of Annual Noise of BDS-3 Satellite New Rubidium Clock.

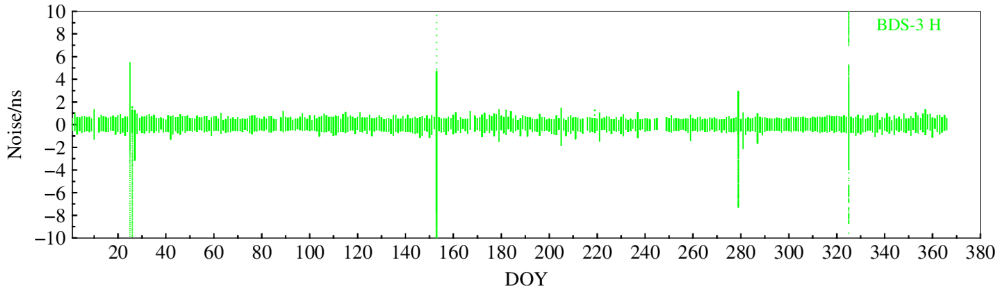

Figure 3: Time Series of Annual Noise of BDS-3 Satellite Hydrogen Clock.

From the above three figures, it is evident that the BDS-2 rubidium clock exhibits relatively high noise level with significant fluctuation and a certain periodic trend. In contrast, the BDS-3 new rubidium clock demonstrates lower noise level. During the early period (DOY 40 to 60), there is a moderate degree of volatility, but overall, the noise level is lower and stability is higher compared to the BDS-2 rubidium clock. The BDS-3 hydrogen clock exhibits the lowest noise level with minimal fluctuation. Presenting smaller noise level and higher noise stability compared to the BDS-3 new rubidium clock.

Table 1: Statistics of Annual Noise of BDS Satellite Clock.

BDS-2 R		BDS-3 R		BDS-3 H	
PRN	**Noise (ns)**	**PRN**	**Noise (ns)**	**PRN**	**Noise (ns)**
C01	0.74	C19	0.70	C25	0.16
C02	2.29	C20	0.21	C26	0.14
C03	0.72	C21	0.85	C27	0.15
C04	0.77	C22	0.22	C28	0.16
C05	0.80	C23	0.48	C29	0.17
C06	0.86	C24	1.43	C30	0.20
C07	0.86	C32	0.22	C34	0.15
C08	0.75	C33	1.82	C35	0.43
C09	0.65	C36	0.17	C38	0.22
C10	0.81	C37	1.65	C39	0.15
C11	0.61	C41	0.20	C40	0.26
C12	0.49	C42	0.17	C43	0.13
C13	0.74			C44	0.23
C14	0.32			C45	0.18
C16	0.57			C46	0.14
Mean	0.80		0.68		0.19

Table 1 provides the annual RMS value of the noise for each BDS satellite. The statistics in Table 1 reveal that satellite C02 of BDS-2 exhibits significantly lower fitting precision compared to other BDS-2 satellites, with a fitting precision of 2.29 ns. This value is an order of magnitude higher than the mean RMS of the fitting residuals for all BDS-2 rubidium atomic clocks. Within the BDS-3 new rubidium clock, satellites C24, C33, and C37 demonstrate poorer fitting precision relative to other BDS-3 new rubidium clocks. Similarly, the RMS values of the fitting residuals for these three satellites are an order of magnitude higher than the mean RMS of the fitting residuals for all BDS-3 new rubidium atomic clocks. In contrast, all BDS-3 hydrogen clocks exhibit robust fitting precision, with the RMS value of the fitting residuals for each hydrogen clock on BDS-3 satellite being on the same order of magnitude as the mean RMS of the fitting residuals for all BDS-3 hydrogen atomic clocks. Notably, satellite C43 within the BDS-3 hydrogen clock has the lowest annual noise level, achieving an RMS value of 0.13 ns, and it also possesses the lowest noise level among all BDS satellite clocks. The annual average RMS values for BDS-2 rubidium clock, BDS-3 new rubidium clock, and BDS-3 hydrogen clock are 0.80 ns,0.68 ns, and 0.19 ns, respectively. Compared to BDS-2 rubidium clock, the enhancements in fitting precision for BDS-3 new rubidium clock and BDS-3 hydrogen clock are 15.00% and 76.25%, respectively.

Satellite Clock Drift Analysis

Taking the daily frequency drift of each BDS satellite as the vertical axis and the DOY as the horizontal axis, and creating Figures 4, 5, and 6. These figures represent the annual time series of frequency drift for BDS satellites, where Figure 4 corresponds to BDS-2 rubidium clock, Figure 5 corresponds to BDS-3 new rubidium clock, and Figure 6 corresponds to BDS-3 hydrogen clock. Table 2 presents the annual RMS value of the frequency drift for each BDS satellite clock, providing a statistical overview of the annual frequency drift.

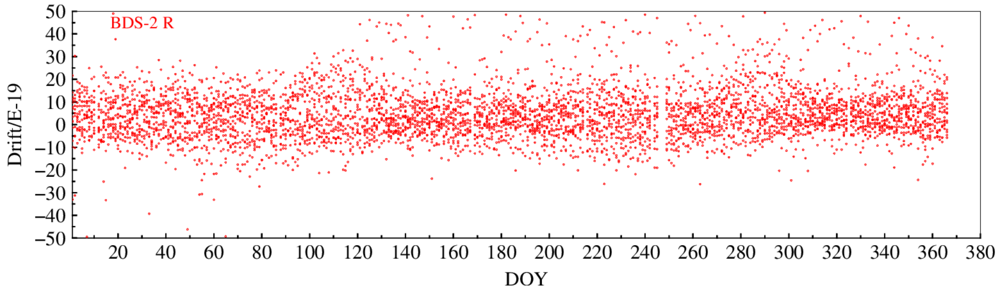

Figure 4: Time Series of Annual Frequency Drift of BDS-2 Satellite Rubidium Clock.

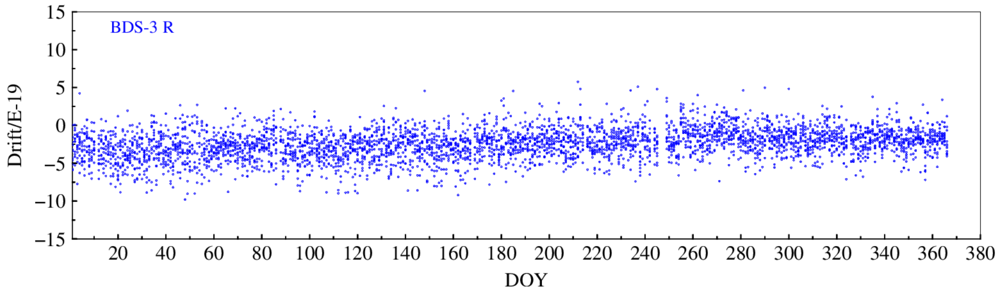

Figure 5: Time Series of Annual Frequency Drift of BDS-2 Satellite New Rubidium Clock.

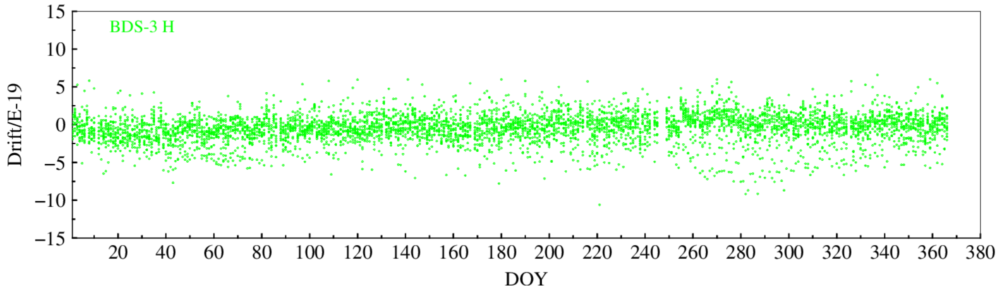

Figure 6: Time Series of Annual Frequency Drift of BDS-2 Satellite Hydrogen Clock.

From the above three figures, it is evident that BDS-2 rubidium clock exhibits a wide range of frequency drift, lower precision, and high volatility. Additionally, there is an upward trend away from zero, indicating a significant systematic bias. In comparison, BDS-3 new rubidium clock demonstrates a narrower frequency drift range and higher precision than BDS-2 rubidium clock. But it still shows a slight downward deviation from zero, suggesting the presence of minor systematic bias. BDS-3 hydrogen clock, exhibits the smallest frequency drift ranges, the most concentrated drift distributions, the highest precision, and no noticeable deviation from zero, indicating the absence of significant systematic biases.

Table 2: Statistics of Annual Frequency Drift of BDS Satellite Clock.

BDS-2 R		**BDS-3 R**		**BDS-3 H**	
PRN	**Drift (10^{-19})**	**PRN**	**Drift (10^{-19})**	**PRN**	**Drift (10^{-19})**
C01	10.61	C19	2.70	C25	2.13
C02	44.70	C20	3.34	C26	1.12
C03	10.96	C21	3.11	C27	1.10
C04	16.76	C22	1.60	C28	1.33
C05	7.66	C23	3.70	C29	1.35
C06	10.48	C24	2.31	C30	2.24
C07	13.08	C32	2.48	C34	1.04
C08	7.79	C33	4.14	C35	2.03
C09	8.49	C36	2.08	C38	3.71
C10	12.99	C37	4.44	C39	2.18
C11	4.41	C41	3.16	C40	1.54
C12	4.96	C42	3.10	C43	1.36
C13	8.47			C44	2.70
C14	7.89			C45	1.56
C16	4.30			C46	1.16
Mean	11.57		3.01		1.77

Since satellite clock drift value is inherent and cannot be adjusted, it can effectively reflect the degree of atomic clock aging. By the data from Table 2, it is observed that the annual average frequency drift value of BDS-2 satellite rubidium clock is on the order of 10^{-18}. Given that BDS-2 satellite clock has been in operation for a longer period, it exhibits more pronounced aging effect, resulting in larger drift value.

Satellites C02, C04, C07, and C10 exhibit frequency drift values exceeding the average frequency drift value of BDS-2 rubidium clock. This is likely attributable to their earlier launch dates, which have led to more significant aging of their onboard atomic clocks. Conversely, the frequency drift value of the later-launched satellite C16 is markedly better than those of the other BDS-2 satellites' onboard rubidium atomic clocks.

Among the BDS-3 new rubidium atomic clocks, satellite C33 exhibits the highest frequency drift value of 4.14×10^{-19}, while satellite C22 has the lowest at 1.60×10^{-19}. For the BDS-3 hydrogen atomic clock, satellite C38 shows the highest frequency drift value of 3.71×10^{-19}, and satellite C27 has the lowest at 1.10×10^{-19}. These observations indicate that BDS-3 hydrogen clock has both lower maximum and minimum frequency drift values compared to BDS-3 new rubidium clock.

Table 2 also reveals that the frequency drift of BDS-3 satellite clock is on the order of 10^{-19}, compared to 10^{-18} for BDS-2 satellites. Moreover, the annual average RMS value of frequency drift of BDS-3 hydrogen atomic clock is smaller than that of BDS-3 new rubidium atomic clock. Specifically, the average annual RMS values of frequency drift are 11.57×10^{-19} for BDS-2 rubidium clock, 3.01×10^{-19} for BDS-3 new rubidium clock, and 1.57×10^{-19} for BDS-3 hydrogen clock. Relative to BDS-2 rubidium clock, the improvements in frequency drift precision for BDS-3 new rubidium and hydrogen clocks are 73.98% and 84.70%, respectively. These enhancements are primarily due to the superior performance of the BDS-3 new rubidium and hydrogen atomic clocks and the fact that BDS-3 satellites were launched later, thereby avoiding severe clock aging issues.

Satellite Clock Stability Analysis

To evaluate the stability levels of different BDS atomic clocks, the PRNs of the BDS satellites are plotted on the horizontal axis, while the annual RMS values of satellite stability are depicted on the vertical axis. Figures 7, 8, and 9 illustrate the annual RMS values for one thousand seconds stability, ten thousand seconds stability, and daily stability for each satellite of BDS, respectively. Table 3 presents the statistical results of the annual RMS values of frequency stability of different BDS satellite atomic clocks.

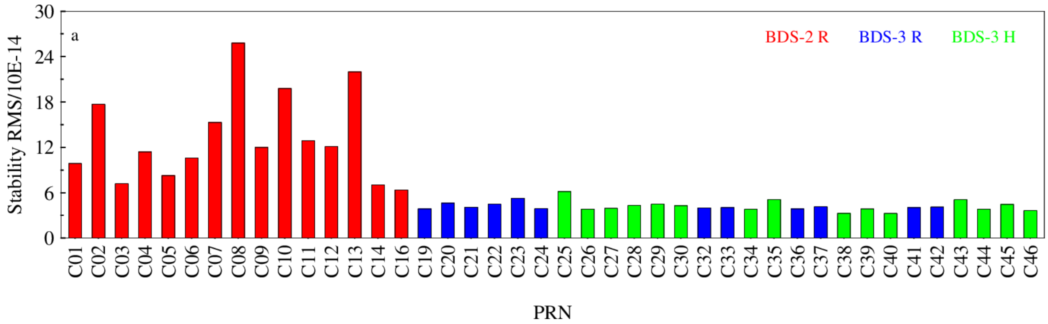

Figure 7: Statistics of Annual One Thousand Seconds Stability of BDS Satellite Clock.

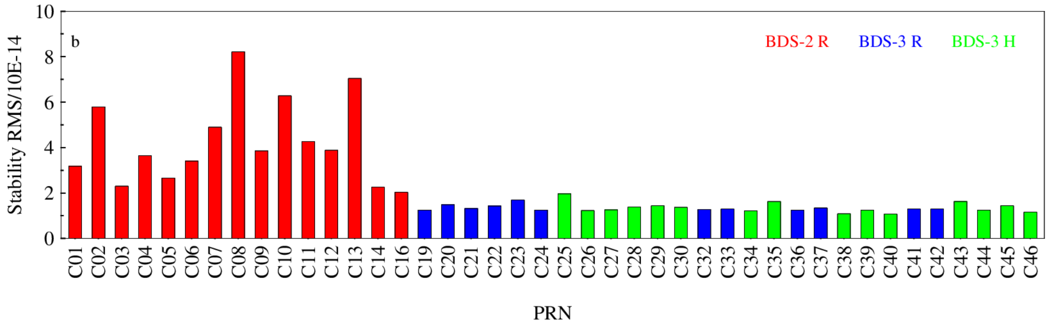

Figure 8: Statistics of Annual Ten Thousand Seconds Stability of BDS Satellite Clock.

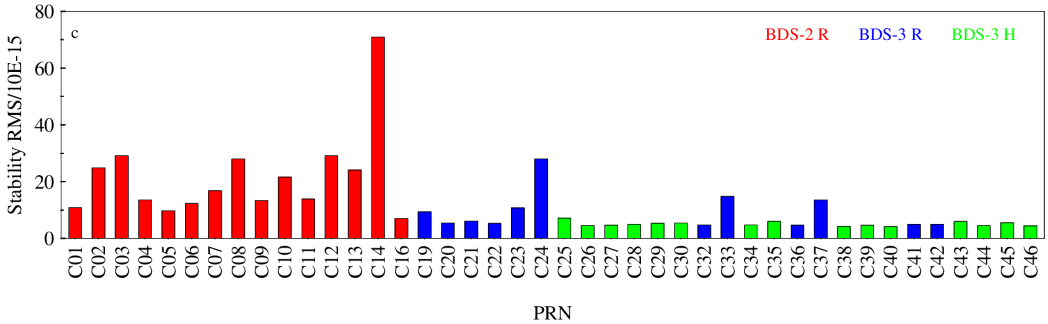

Figure 9: Statistics of Annual Daily Stability of BDS Satellite Clock.

From the three figures, the one thousand seconds stability of BDS-2 rubidium clock is mostly on the order of 10^{-13}, while the ten thousand seconds and daily stabilities are generally within the 10^{-14} range. In contrast, BDS-3 atomic clocks' one thousand seconds and ten thousand seconds stabilities are around the 10^{-14} level, with daily stabilities mostly achieving the 10^{-15} range.

Combining the statistical information from Table 3, it can be concluded that the BDS-3 hydrogen clock demonstrates superior stability compared to both the BDS-2 rubidium clock and the BDS-3 new rubidium clock, with the BDS-2 rubidium clock exhibiting the poorest stability. Specifically, the one thousand seconds stability and the daily stability precisions of BDS-3 new rubidium and hydrogen clocks surpass those of the BDS-2 rubidium clocks by one order of magnitude. The ten thousand seconds stability differences between BDS-2 and BDS-3 atomic clocks are relatively minor. Additionally, the one thousand seconds stability and ten thousand seconds stability precisions of BDS-3 hydrogen atomic clock are essentially consistent with those of BDS-3 rubidium atomic clock. However, the daily stability of BDS-3 hydrogen clock, which operates at the 10^{-15} level, significantly outperforms that of BDS-2 rubidium clock. And it is markedly more precise than that of the BDS-3 new rubidium clock, with an improvement ratio of 45.64%.

Table 3: Statistics of Annual Stability of BDS Satellite Clock.

Satellite Clock	**One Thousand (10^{-14})**	**Ten Thousand (10^{-14})**	**Daily (10^{-15})**
BDS-2 R	13.22	4.25	21.69
BDS-3 R	4.22	1.36	9.40
BDS-3 H	4.20	1.35	5.11

In the daily stability statistics, the rubidium clock of satellite C14 in the BDS-2 constellation exhibits relatively poor stability, with an annual daily stability RMS value of 7.09×10^{-14} and an annual ten thousand seconds stability RMS value of 2.26×10^{-14}. The daily stability of this satellite is inferior to its ten thousand seconds stability, which may be attributed to the instability of the satellite clock data.

Relative to the BDS-2 rubidium clock, the BDS-3 new rubidium and hydrogen clocks achieve precision enhancements in one thousand seconds stability by 68.08% and 68.23%, respectively. In ten thousand seconds stability, the precision improvements for BDS-3 rubidium and hydrogen clocks are 68.00% and 68.24%, respectively. Regarding daily stability, the precision enhancements for BDS-3 rubidium and hydrogen clocks are 56.67% and 76.44%, respectively.

Satellite Clock Error Prediction Accuracy and Stability Analysis

To gain an intuitive understanding of the prediction accuracy and stability of the three types of BDS satellite atomic clocks under different prediction models and varying prediction durations, prediction residuals were plotted with prediction duration on the horizontal axis and prediction residual on the vertical axis. Figures 10, 11, and 12 present the time series of prediction residuals for 12 hours on the DOY 152 of 2024. From the three figures, it is apparent that among the QP, GM, and ARIMA models, the ARIMA model yields the most optimal prediction results.

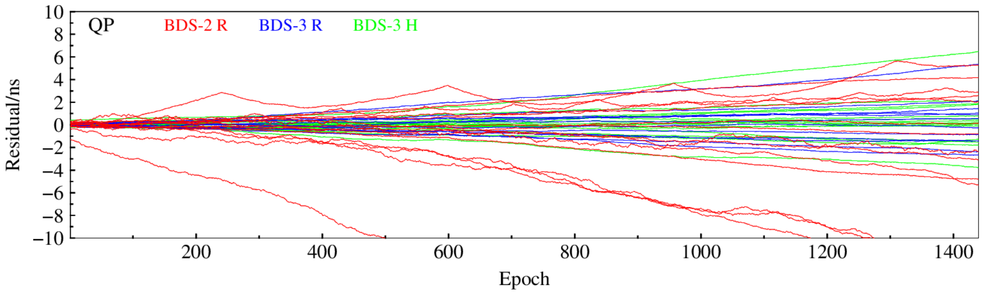

Figure 10: Prediction Residual Statistics of BDS Satellite Clock of QP.

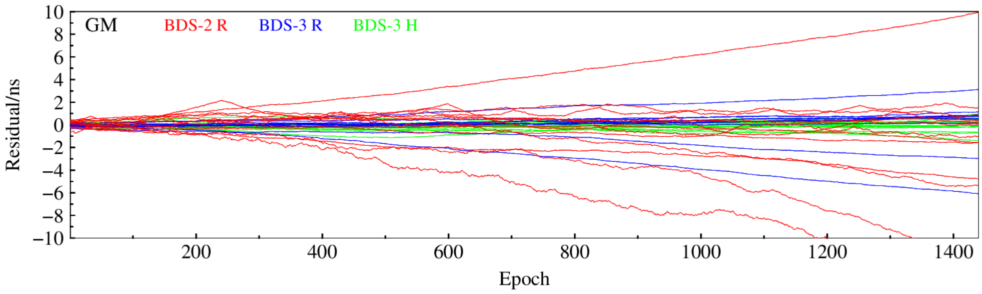

Figure 11: Prediction Residual Statistics of BDS Satellite Clock of GM.

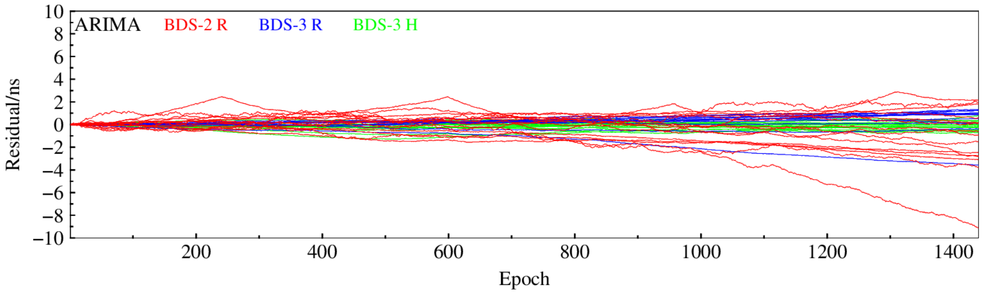

Figure 12: Prediction Residual Statistics of BDS Satellite Clock of ARIMA.

Tables 4, 5, and 6 report the mean RMS values of the prediction residuals for the three models across different prediction durations within a 7 days (DOY 146 to 152) period, thereby assessing the prediction accuracy of each model. Concurrently, Tables 7, 8, and 9 provide the mean standard deviation (STD) values of the prediction residuals for the three models across different prediction durations within a 7 days (DOY 146 to 152) period, evaluating the prediction stability. Analysis of the aforementioned 6 tables reveals that the ARIMA model achieves mean RMS values of 0.85 ns for 12 hours prediction, 0.51 ns for 6 hours prediction, and 0.35 ns for 3 hours prediction, thereby demonstrating superior prediction accuracy relative to the other two models. In terms of prediction stability, the ARIMA model achieves mean STD values of 0.75 ns for 12 hours prediction, 0.47 ns for 6 hours prediction, and 0.31 ns for 3 hours prediction, further underscoring its optimal stability performance compared to the QP and GM models.

For the entire BDS satellite constellation, the GM model exhibits slightly better prediction accuracy and stability than the QP model. For BDS-2 rubidium clock and BDS-3 hydrogen clock, the GM model's prediction accuracy and stability are superior to those of the QP model. However, for BDS-3 new rubidium clock, the QP model significantly outperforms the GM model in both prediction accuracy and stability in 3 hours, 6 hours, and 12 hours durations. Overall, the RMS values (with the mean of the three prediction models) of the prediction residuals of the BDS satellite clock in 3 hours, 6 hours, and 12 hours are 0.65 ns, 1.13 ns, and 2.38 ns. The STD values of the prediction residuals are 0.61 ns, 1.08 ns, and 2.29 ns, respectively. From the statistical results of the 6 tables above, it can be seen that the RMS value of the model prediction accuracy and the STD value of the prediction stability indicate that the prediction accuracy of the three models is mainly affected by the prediction stability.

Table 4: Statistics of Prediction Accuracy for BDS Satellite Clock in 3 Hours.

Model	**3 h RMS (ns)**			
	BDS-2 R	**BDS-3 R**	**BDS-3 H**	**Mean**
QP	1.43	0.55	0.46	0.81
GM	1.20	0.89	0.25	0.78
ARIMA	0.64	0.21	0.19	0.35
Mean	1.09	0.55	0.30	0.65

Table 5: Statistics of Prediction Accuracy for BDS Satellite Clock in 6 Hours.

Model	**6 h RMS (ns)**			
	BDS-2 R	**BDS-3 R**	**BDS-3 H**	**Mean**
QP	2.72	0.99	0.80	1.50
GM	2.21	1.59	0.31	1.37
ARIMA	0.97	0.31	0.26	0.51
Mean	1.97	0.96	0.46	1.13

Table 6: Statistics of Prediction Accuracy for BDS Satellite Clock in 12 Hours.

Model	**12 h RMS (ns)**			
	BDS-2 R	**BDS-3 R**	**BDS-3 H**	**Mean**
QP	6.08	2.03	1.77	3.29
GM	5.10	3.58	0.34	3.01
ARIMA	1.64	0.58	0.33	0.85
Mean	4.27	2.06	0.81	2.38

For the entire BDS satellite constellation, the QP, GM, and ARIMA models can achieve prediction accuracies of 0.81 ns, 0.78 ns, and 0.35 ns, respectively, within 3 hours. The prediction stability within 3 hours can reach 0.79 ns, 0.74 ns, and 0.31 ns, respectively. The corresponding improvement ratios of ARIMA model to QP and GM models in prediction accuracy are 56.80% and 55.13%, respectively. The improvement ratios of prediction stability are 60.76% and 58.11%, respectively. Similarly, when the prediction duration is 6 hours, the improvement ratios of ARIMA model to QP and GM models in prediction accuracy are 66.00% and 62.78%, respectively. The improvement ratios of prediction stability are 67.58% and 64.66%, respectively. It can also be concluded that when the prediction duration is 12 hours, the improvement ratios of ARIMA model to QP and GM models in prediction accuracy are 74.16% and 71.76%, respectively. The improvement ratios of prediction stability are 76.26% and 74.66%, respectively. It can be observed that for the entire BDS satellite constellation, as the prediction duration increases, the ratios of improvement in ARIMA model prediction accuracy and prediction stability will also increase.

Table 7: Statistics of Prediction Stability for BDS Satellite Clock in 3 Hours.

Model	3 h STD (ns)			
	BDS-2 R	BDS-3 R	BDS-3 H	Mean
QP	1.38	0.55	0.43	0.79
GM	1.13	0.86	0.24	0.74
ARIMA	0.64	0.15	0.14	0.31
Mean	1.05	0.52	0.27	0.61

Table 8: Statistics of Prediction Stability for BDS Satellite Clock in 6 Hours.

Model	6 h STD (ns)			
	BDS-2 R	BDS-3 R	BDS-3 H	Mean
QP	2.60	0.98	0.76	1.45
GM	2.15	1.55	0.30	1.33
ARIMA	0.96	0.23	0.23	0.47
Mean	1.90	0.92	0.43	1.08

Table 9: Statistics of Prediction Stability for BDS Satellite Clock in 12 Hours.

Model	12 h STD (ns)			
	BDS-2 R	BDS-3 R	BDS-3 H	Mean
QP	5.80	2.03	1.66	3.16
GM	5.07	3.49	0.33	2.96
ARIMA	1.56	0.39	0.31	0.75
Mean	4.14	1.97	0.77	2.29

For ARIMA model, the prediction accuracies for BDS-2 rubidium clock, BDS-3 new rubidium clock, and BDS-3 hydrogen clock in a 12 hours prediction duration reach 1.64 ns, 0.58 ns, and 0.33 ns, respectively. Corresponding to prediction accuracy improvement ratios of 64.63% and 79.88% for BDS-3 new rubidium and hydrogen clocks relative to BDS-2 rubidium clock. The prediction stabilities for those atomic clocks in the 12 hours prediction duration are 1.56 ns, 0.39 ns, and 0.31 ns, with improvement ratios of 75.00% and 80.13% for BDS-3 new rubidium and hydrogen clocks relative to BDS-2 rubidium clock. Similarly, when the prediction duration is 6 hours, the improvement ratios of the BDS-3 new rubidium clock and BDS-3 hydrogen clock compared to the BDS-2 rubidium clock in terms of prediction accuracy are 68.04% and 73.20%, respectively, and the improvement ratios of prediction stability are 76.04% and 76.04%, respectively. It can also be concluded that when the prediction duration is 3 hours, the improvement ratios of the prediction accuracy of BDS-3 new rubidium clock and BDS-3 hydrogen clock relative to BDS-2 rubidium clock are 67.19% and 70.31%, respectively, and the improvement ratios of prediction stability are 76.56% and 78.13%, respectively. For BDS-3 hydrogen clock, the improvement ratio in prediction accuracy relative to BDS-2 rubidium clock increases with longer prediction durations.

Among the three types of BDS satellite atomic clocks, the BDS-3 hydrogen clock consistently exhibits the highest prediction accuracy and stability across all three prediction models. The BDS-3 new rubidium clock outperforms the BDS-2 rubidium clock in both prediction accuracy and stability.

In the process of positioning applications, BDS satellite clock error will have a significant impact on the signal in space range error (SISRE) of the satellite (Dong et al., 2024). Therefore, it is necessary to refine the basic clock error model to meet the requirements of high precision positioning.

Conclusions

This study analyzes the BDS satellite clock noise, frequency drift, frequency stability, based on one year of WHU precise clock error data. Based on 7 days fitted data, analyze the prediction results of BDS satellite clock error using QP, GM, and ARIMA models. The findings provide valuable insights and reference for understanding the performance of BDS satellite and refining the BDS satellite clock error model.

The BDS-3 hydrogen clock exhibits the lowest annual noise level, with annual RMS values of 0.19 ns, compared to 0.80 ns for BDS-2 rubidium clock and 0.68 ns for BDS-3 new rubidium clock. Relative to the BDS-2 rubidium clock, the BDS-3 new rubidium and hydrogen clocks have been reduced in noise by 15.00% and 76.25%, respectively.

The annual RMS values of frequency drift are 11.57×10^{-19} for BDS-2 rubidium clock, 3.01×10^{-19} for BDS-3 new rubidium clock, and 1.57×10^{-19} for BDS-3 hydrogen clock. Compared to the BDS-2 rubidium clock, the BDS-3 new rubidium and hydrogen clocks demonstrate significant enhancements in frequency drift precision, with improvement ratios of 73.98% and 84.70%, respectively.

The BDS-3 hydrogen clock exhibits superior frequency stability, with one thousand seconds stability exceeding BDS-2 rubidium clock by one order of magnitude and its daily stability reaching the 10^{-15} level. Specifically, the daily stability precision of the BDS-3 hydrogen clock improves by 76.44% compared to BDS-2 rubidium clock and by 45.64% compared to

BDS-3 new rubidium clock.

The BDS-3 atomic clocks outperform the BDS-2 atomic clock in both prediction accuracy and stability, with BDS-3 hydrogen clock achieving the best results. As the prediction duration increases, the improvement ratio in prediction accuracy for BDS-3 hydrogen clock relative to BDS-2 rubidium clock also increases. Even at longer prediction durations, BDS-3 hydrogen clock maintains superior prediction accuracy and stability, indicating that higher-performing atomic clock achieves greater prediction precision.

Among the three prediction models, the ARIMA model yields the most optimal results, providing the best prediction accuracy and stability. For the entire BDS constellation, the QP model does not perform as well as the GM model in terms of prediction accuracy and stability. However, for BDS-3 new rubidium clock, the QP model surpasses the GM model in both prediction accuracy and stability. Additionally, within the entire BDS satellite constellation, the improvement ratios for prediction accuracy and stability using the ARIMA model relative to the QP and GM models increase with longer prediction durations.

Acknowledgments

The WHU is greatly acknowledged for providing BDS precise clock products.

References

Allan, D., & Levine, J., (2016). A Historical Perspective on the Development of the Allan Variances and their Strengths and Weaknesses. *IEEE TRANSACTIONS ON ULTRASONICS, FERROELECTRICS, AND FREQUENQY CONTROL*, *63*(4), 513-519. https://doi.org/10.1109/TUFFC.2016.2524687

Dong, Z.H., & Zhang, S.L., (2024). SISRE of BDS-3 MEO: Evolution as Well as Comparison between D1 and B-CNAV (B-CNAV1, B-CNAV2) Navigation Messages. *Remote Sens*, 16, 484. https://doi.org/10.3390/rs16030484

Guo, S.R., Cai, H.L., Meng, Y.N., Geng, C.J., Jia, X.L., Mao, Y., Geng, T., Yao, Y.N., Zang, H.J., & Xie, X., (2019). BDS-3 RNSS technical characteristics and service performance. *Acta Geodaetica et Cartographica Sinica*, *48*(7), 810-821. https://doi.org/10.11947/j.AGCS.2019.20190091

Hauschild, A., Montenbruck, O., & Steigenberger, P., (2013). Short-term analysis of GNSS clocks. *GPS Solut*, 17, 295-307. https://doi.org/10.1007/s10291-012-0278-4

Huang, G.W., Yu, H., Guo, H.R., Zhang, J.Q., Fu W.J., & Tian J., (2017). Analysis of the Mid-long Term Characterization for BDS On-orbit Satellite Clocks. *Geomatics and*

Information Science of Wuhan University, *42*(7), 982-987. https://doi.org/10.13203/j.whugis20140827

Huang, G.W., Cui, B.B., Zhang, Q., Fu, W.J., & Li, P.L., (2018). An Improved Predicted Model for BDS Ultra-Rapid Satellite Clock Offsets. *Remote Sens*, 10, 60. https://doi.org/10.3390/rs10010060

Jiang, Q.C., Zhao, L.L., Liu W.K., & Li, Z.Q., (2019). Long-Term Performance Assessment of BD-2 On-Board Atomic Clocks. *Journal of Geodesy and Geodynamics*, *39*(10), 1047-1052. https://doi.org/10.14075/j.jgg.2019.10.012

Kan, H.Y., Hu, Z.G., Lv, Y.F., Xie, X., Zhou, R.Y., & Zhao, Q.L., (2021). Performance Evaluation of BDS-3 Spaceborne Atomic Clock Using Different Time Synchronization Systems. *Geomatics and Information Science of Wuhan University*, *48*(4), 604-610. https://doi.org/10.13203/j.whugis20210286

Li, C., Dang, Y.M., & Gu, S.Z., (2016). Prediction of GLONASS satellite clock error based on grey model. *Journal of Navigation and Positioning*, *4*(4), 24-29. https://doi.org/10.16547/j.cnki.10-1096.20160405

Mao, Y., Chen, J.P., Dai, W., Jia, & X.L., (2011). Analysis of On-board Atomic Clock Stability Influences. *Geomatics and Information Science of Wuhan University*, *36*(10), 1182-1185. https://doi.org/10.13203/j.whugis2011.10.003

Mao, Y., Wang, Q.X., Hu, C., Yang, H.Y., & Zhang, M.B., (2020). Analysis of the Characterization for BDS-3 Satellite Clock Error. *Geomatics and Information Science of Wuhan University*, *45*(1), 53-60. https://doi.org/10.13203/j.whugis20180224

Meng, C.X., Wu, D., & Lei, Y., (2022). BP Neural Network for Satellite Clock Bias Prediction Based on Sparrow Search Algorithm. *Journal of Geodesy and Geodynamics*, *42*(2), 125-131. https://doi.org/10.14075/j.jgg.2022.02.004

Panfilo, G., & Tavella, P., (2008). Atomic clock prediction based on stochastic differential equations. *Metrologia*, *45*(6), S108. https://doi.org/10.1088./0026-1394/45/6/S16

Senior, K.L., Ray, J.R., & Beard, R.L., (2008). Characterization of periodic variations in the GPS satellite clocks. *GPS Solut*, 12, 211-225. https://doi.org/10.1007/s10291-008-0089-9

Wang, L., & Bi, X.H., (2021). Risk assessment of knowledge fusion in an innovation ecosystem based on a GA-BP neural network. *Cognitive Systems Research*, *66*(46), 201-210. https://doi.org/10.1016/j.cogsys.2020.12.006

Wang, N., Wang, Y.P., Li, L.Y., Zhai, S.F., & Lv, Z.P., (2017). Stability Analysis of the Space-borne Atomic Clock Frequency for BDS. *Geomatics and Information Science of Wuhan University*, *42*(9), 1256-1262. https://doi.org/10.13203/j.whugis20150806

Xi, C., Cai, C.L., Li, S.M., Li, X.H., Li, Z.B., & Deng, K.Q., (2014). Long-term Clock Bias Prediction Based on An ARMA Model. *Chinese Astronomy and Astrophysics*, *38*(3), 342-354. https://doi.org/10.1016/j.chinastron.2014.07.010

Zheng, Z.Y., Chen, Y.Q., & Lu, X.S., (2008). An Improved Grey Model for the Prediction of Real-Time GPS Satellite Clock Bias. *ACTA ASTRONOMICA SINICA*, *49*(3), 306-319. https://doi.org/10.15940/j.cnki.0001-5245.2008.03.012